

Multi-contrast focal modulation microscopy for in vivo imaging of thick biological tissues

Nanguang Chen* and Guangjun Gao

Department of Bioengineering, Faculty of Engineering, National University of Singapore, Singapore 117576, Singapore

*biecng@nus.edu.sg

Abstract: In vivo high resolution imaging of biological tissues is desirable for a wide range of biomedical applications. Recently focal modulation microscopy (FMM) has been developed and an imaging depth comparable to multi-photon microscopy (MPM) and optical coherence microscopy (OCM) has been achieved. Here we report the first focal modulation microscope that is capable of performing real-time fluorescence and scattering imaging simultaneously on thick biological tissues. A novel spatiotemporal phase modulator (STPM) has been designed and integrated into such a microscope to achieve high performances in terms of imaging speed, contrast, effective spatial resolution, signal to noise ratio, and compatibility with multiple excitation wavelengths.

©2012 Optical Society of America

OCIS codes: (170.0110) Imaging systems; (110.0180) Microscopy; (180.5810) Scanning microscopy.

References and links

1. S. M. Ameer-Beg, P. R. Barber, R. J. Hodgkiss, R. J. Locke, R. G. Newman, G. M. Tozer, B. Vojnovic, and J. Wilson, "Application of multiphoton steady state and lifetime imaging to mapping of tumour vascular architecture in vivo," *Proc. SPIE* **4620**, 85–95 (2002).
2. U. Dirnagl, U. Lindauer, A. Them, W. Pfister, K. M. Einhaupl, and A. Villringer, "Subsurface microscopic visualization of brain-tissue in-vivo—present, problems and prospects," *Micron* **24**(6), 611–622 (1993).
3. F. Helmchen and W. Denk, "Deep tissue two-photon microscopy," *Nat. Methods* **2**(12), 932–940 (2005).
4. D. Huang, E. A. Swanson, C. P. Lin, J. S. Schuman, W. G. Stinson, W. Chang, M. R. Hee, T. Flotte, K. Gregory, C. A. Puliafito, and J. G. Fujimoto, "Optical coherence tomography," *Science* **254**(5035), 1178–1181 (1991).
5. W. M. Petroll, J. V. Jester, and H. D. Cavanagh, "In vivo confocal imaging: general principles and applications," *Scanning* **16**(3), 131–149 (1994).
6. P. Timpson, E. J. McGhee, and K. I. Anderson, "Imaging molecular dynamics in vivo—from cell biology to animal models," *J. Cell Sci.* **124**(17), 2877–2890 (2011).
7. I. Tomo, S. Le Calvez, H. Maier, J. Boutet de Monvel, A. Fridberger, and M. Ulfendahl, "Imaging the living inner ear using intravital confocal microscopy," *Neuroimage* **35**(4), 1393–1400 (2007).
8. N. Wuyts, J. C. Palauqui, G. Conejero, J. L. Verdeil, C. Granier, and C. Massonnet, "High-contrast three-dimensional imaging of the Arabidopsis leaf enables the analysis of cell dimensions in the epidermis and mesophyll," *Plant Methods* **6**(1), 17 (2010), doi:10.1186/1746-4811-6-17, <http://www.plantmethods.com/content/6/1/17>.
9. S. Khoshyomn, P. L. Penar, W. J. McBride, and D. J. Taatjes, "Four-dimensional analysis of human brain tumor spheroid invasion into fetal rat brain aggregates using confocal scanning laser microscopy," *J. Neurooncol.* **38**(1), 1–10 (1998).
10. M. Gu and C. J. R. Sheppard, "Three-dimensional image-formation in confocal fluorescence microscopy," *Proc. SPIE* **1660**, 188–198 (1992).
11. C. E. Miller, R. P. Thompson, M. R. Bigelow, G. Gittinger, T. C. Trusk, and D. Sedmera, "Confocal imaging of the embryonic heart: how deep?" *Microsc. Microanal.* **11**(03), 216–223 (2005).
12. J. A. Izatt, M. D. Kulkarni, H.-W. Wang, K. Kobayashi, and M. V. Sivak, "Optical coherence tomography and microscopy in gastrointestinal tissues," *IEEE J. Sel. Top. Quantum Electron.* **2**(4), 1017–1028 (1996).
13. N. G. Chen, C. H. Wong, and C. J. R. Sheppard, "Focal modulation microscopy," *Opt. Express* **16**(23), 18764–18769 (2008), <http://www.opticsinfobase.org/oe/abstract.cfm?URI=oe-16-23-18764>.
14. S. P. Chong, C. H. Wong, C. J. R. Sheppard, and N. G. Chen, "Focal modulation microscopy: a theoretical study," *Opt. Lett.* **35**(11), 1804–1806 (2010).
15. G. J. Gao, S. P. Chong, C. J. R. Sheppard, and N. G. Chen, "Considerations of aperture configuration in focal modulation microscopy from the standpoint of modulation depth," *J. Opt. Soc. Am. A* **28**(4), 496–501 (2011).

1. Introduction

Scattering imposes a fundamental challenge for diffraction limited high resolution imaging of thick biological tissues with light microscopy. Traditional wide-field microscope can only deal with mechanically sectioned samples a few microns in thickness. New light microscopy techniques have been emerging and evolving rapidly since lasers, high sensitivity photodetectors, and modern electronics started to play a role in this field [1–8]. Optical sectioning was firstly achieved with confocal microscopy (CM), which relies on confocal point detection to reject out of focus background [2,5,9,10]. CM allows sub-cellular layer by layer imaging of tissues up to 200 μm in depth [11].

Nonlinear interactions between light and matter provide a very effective mechanism for selectively exciting molecules in the focal volume [1,3]. In Multi-photon microscopy (MPM), an imaging depth of 600–800 μm can be achieved with an average source power of 1 Watt, as a result of slower signal attenuation due to reduced scattering (longer excitation wavelength) and localized absorption [3]. MPM is also attractive because of localized photochemistry and reduced photobleaching. However, MPM is a rather expensive technique that requires femtosecond or picosecond pulsed lasers. There are also a few technical disadvantages as well. Two-photon absorption spectra are generally much broader than their single-photon counterparts. The significantly overlapping absorption spectra make it more difficult to perform multi-fluorophore experiments with multi-photon excitation. In addition, MPM does not detect backscattering, an intrinsic label free contrast mechanism for visualization of microscopic structures.

Optical coherence microscopy (OCM) is a variant of optical coherence tomography (OCT) [4]. It uses a high numerical aperture (NA) objective lens in the sample arm for sub-cellular spatial resolution, at the price of reduced imaging speed. OCM, however, does not enjoy an imaging depth comparable to that of OCT. To the best of our knowledge, the maximal OCM imaging depth reported in literature was about 600 μm , achieved with a large NA (0.65) for a spatial resolution around 1.9 μm [12]. While OCM is a label free imaging method, its incompatibility with fluorescence is a limitation for molecular and functional imaging applications.

Focal modulation microscopy (FMM) is an emerging method for high resolution deep imaging of biological tissues. The basic principle of FMM has been described in our previously publications [13–16]. Briefly, a STPM is inserted into the excitation light path and generates a periodic intensity modulation confined within the focal volume. Emission from the focal volume is modulated at the same frequency, while the background is essentially constant and can be effectively rejected using an appropriate demodulation scheme. An imaging depth up to 600 μm into cartilage has been demonstrated experimentally with the first prototype FMM. While the configuration of the prototype FMM is compatible with most contrast mechanisms, the minimum image acquisition time is far longer than that of a commercial CM, severely limiting its application range.

The key component determining the performance of FMM is the STPM. In the first prototype FMM, the modulator consists of two parallel mirrors, one stationary and another driven by a PZT actuator for periodic phase shifting. Such a STPM can only be operated at a modulation frequency up to a few kHz [13]. In addition, it is very difficult to implement more complex spatial patterns for an optimal modulation depth [15]. More recently we used two acousto-optic modulators (AOMs) to achieve a high modulation frequency of 10 MHz [16]. However, the AOM based STPM needs optical realignment when switching from one excitation wavelength to another. It also suffers from low modulation depth.

Here we report a novel implementation of STPM, which consists of a phase only Electro-optic modulator (EOM) and polarization optics. The EOM provides very high speed (9.85 MHz) temporal phase modulation while the polarization optics spatially separates the

modulated and non-modulated excitation light. Such a modulator is integrated into a commercial confocal microscope to upgrade it into a FMM system. We demonstrate the improved imaging capability and performances using a series of imaging experiments.

2. System design

Figure 1(a) shows the design of a STPM and how it is incorporated in an Olympus FV300 confocal system. The major components of the STPM include linear polarizers, an EOM, and a spatial polarizer. The first polarizer P1 linearly polarizes the excitation light from the FV300 laser unit, which combines the output from three lasers (488 nm, 559 nm, and 633 nm) into a single mode optical fiber. The collimated excitation light passes through P1 and its polarization is maintained at 45 degrees with the horizon. The EOM (EOM-01-10-U, Photonics Technologies) is driven by a high frequency ($f_0 = 9.85$ MHz) sine wave signal so that the horizontal component of the excitation beam is phase modulated. The EOM is followed by a six-zone spatial polarizer, which consists of six segments of colorPol@VIS600BC4 linear polarizer (CODIXX). The polarization direction of each segment is shown in Fig. 1(b). The gray zones represent segments with a vertical polarization direction while the white zones have a horizontal polarization direction. The spatial polarizer is a static component placed centrally in the excitation beam. It selectively passes vertically polarized (non-modulated) or horizontally polarized (modulated) excitation light. Such a spatial separation is determined by the configuration of the spatial polarizer. Complex patterns can be readily implemented. The second polarizer P2 following the spatial polarizer projects the modulated and non-modulated fields onto the same polarization axis so that they can interfere with each other when converging to the focal point.

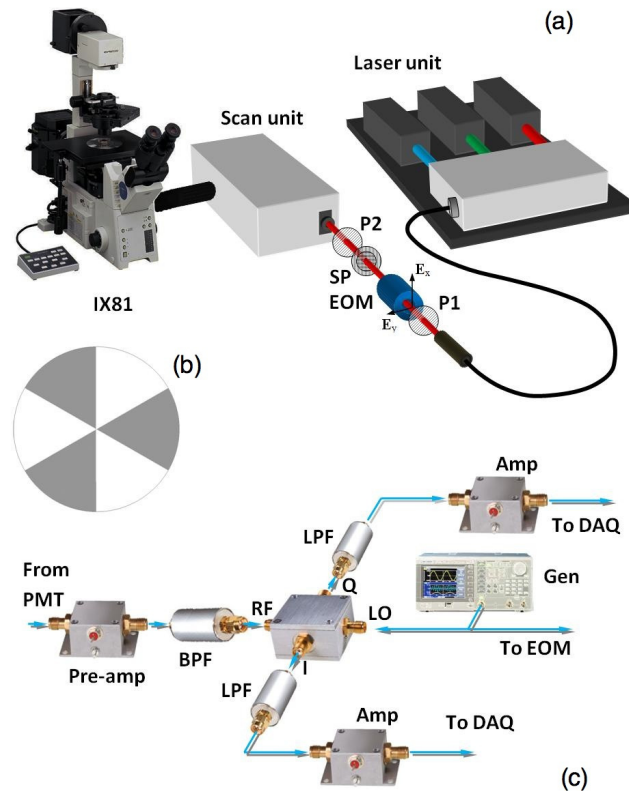


Fig. 1. (a) A STPM is inserted in the excitation light path of an Olympus FV300 confocal microscope for FMM imaging. (b) A six-zone spatial polarizer that selectively passes horizontally polarized light (white zones) or vertically polarized light (gray) zones. (c) Signal processing circuit for demodulation. See the text for details.

The spatiotemporally modulated excitation beam is directed to the entry port of the FV300 scan head, which is attached to an IX81 inverted microscope. The scan head includes two-dimensional scanning mirrors, dichroic mirrors, emission filters, confocal pinholes, and photomultiplier tubes (PMTs). Fluorescence emission and/or reflectance are selected by appropriate dichroic mirrors and emission filters to pass through a pinhole before a PMT. The optoelectric signal from the PMT contains a baseband component and a modulated radio-frequency (RF) component at f_0 . A signal processing circuit shown in Fig. 1(c) is employed for retrieving the in-phase (I) and quadrature-phase (Q) amplitudes of the RF component, which leads to FMM images. The modulated RF component from the PMT is enhanced by the pre-amp and cleaned by a bandpass filter (BPF). An I/Q demodulator mixes the RF signal with a LO signal to generate I and Q baseband signals, which are further conditioned by low-pass filters (LPF's) and baseband amplifiers (Amp's). The amplitude $\sqrt{I^2 + Q^2}$ is computed for FMM imaging, and it is insensitive to additional phase changes due to variable cable length and PMT multistage amplification. The 9.85 MHz output from a functional generator (GEN) is used for both modulation and demodulation. Confocal images are generated simultaneously from the baseband component. At the moment we have only one detection channel upgraded with the demodulation circuit.

3. Imaging experiments and results

Epipremnum Aureum leaves were used as samples to demonstrate the imaging performance of our EOM-STPM based FMM. Fresh leaves were picked immediately before imaging experiments. In each experiment, a small piece of roughly 5mm by 5 mm was cut from a leaf and put in a glass bottom dish (P35G-0-10-C, MatTek Corp.). The leaf top surface was facing down against the glass coverslip. Distilled water was added to the dish for refractive index matching. The microscope was operated in the XYZ mode for acquiring 3D image stacks. The sampling speed was fixed at 8 μ s per pixel and the XY image size was roughly 512 x 512 pixels. A 40x/1.1 water immersion objective lens (441857-9970-000, Carl Zeiss) was used in the imaging experiments.

First of all, we validated the capability of this system for FMM imaging with multiple excitation wavelengths and different contrast mechanisms. Shown in Fig. 2(a) is a merged fluorescence/scattering image of the sample obtained from a depth range of 71-150 μ m. The red channel corresponds to autofluorescence from chloroplasts excited by the 559 nm laser. The green channel is related to cell membranes and intracellular organelles that scatter or reflect the illumination from the red laser (633 nm). It is obvious that the sub-cellular features revealed by both contrast mechanisms were perfectly aligned.

Next, we compared CM and FMM images acquired simultaneously to demonstrate that the latest FMM could provide the same background rejection capability as our previous implementations. Figures 2(b) and 2(d) are en-face and cross-sectional CM images, respectively, from an image depth between 68 μ m to 88 μ m. Remarkably improved contrast and effective spatial resolution can be seen in the corresponding FMM images (Figs. 2(c) and 2(e)). Line profiles taken from the cross-sectional images are compared in Figs. 2(f) and 2(g). Again it is apparent that FMM is advantageous in preserving high spatial frequency components and rejecting background from scattered photons.

The modulation depth of the STPM was measured around 0.5. Compared with the AOM-based modulator, the signal to noise ratio in FMM images has been improved by 6 dB. We plan to test other spatial patterns (such as the six-zone annular aperture) in the future in order to further enhance the signal to noise ratio.

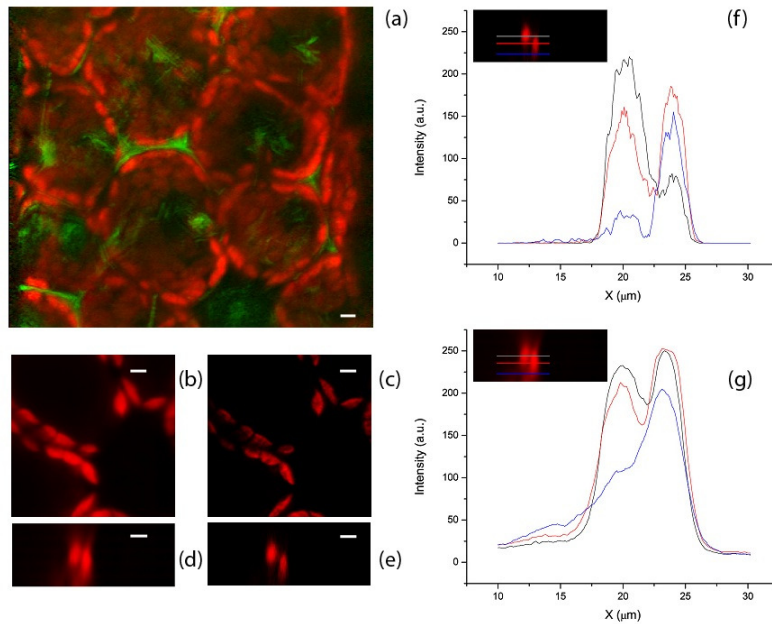


Fig. 2. (a) Merged leaf image (Media 1) from autofluorescence (red) and backscattering/reflectance (green). (b) Autofluorescence chloroplasts *en face* and (d) cross-sectional CM images, respectively, were acquired simultaneously with corresponding FMM images (c) and (e). (f) Line profiles taken along same color lines in the FMM image (e). (g) Line profiles taken along same color lines in the CM image (d). Scale bars: 5 μm .

4. Conclusion

We have developed a real-time focal modulation microscope based on a novel design of spatiotemporal phase modulator. It is essentially compatible with most *in vivo* imaging contrast mechanisms, i.e., single photon fluorescence, multiphoton fluorescence, and scattering/reflection. Although multiphoton microscopy imaging experiments have not been carried out using our FMM, we believe that it should be straightforward to add pulsed excitation light sources to our system.